Institute of Paper Science and Technology
Atlanta, Georgia

IPST TECHNICAL PAPER SERIES

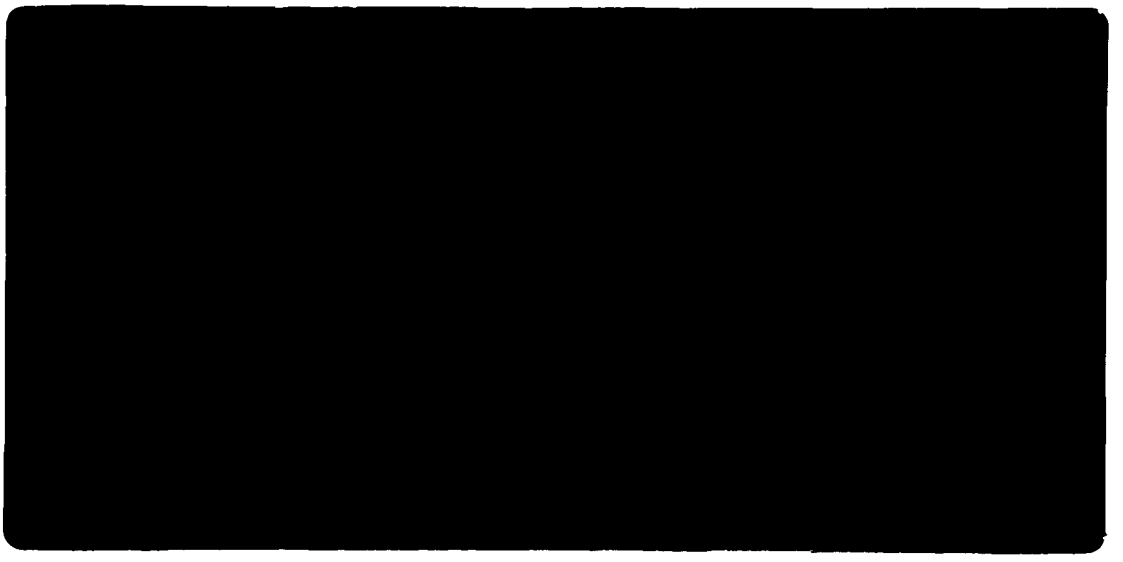

NUMBER 462

SENSITIVITY STUDIES OF IN-FLIGHT BLACK LIQUOR COMBUSTION USING A THREE-DIMENSIONAL COMPUTER MODEL

R.R. HORTON, D.J. SLAYTON, T.M. GRACE, AND T.N. ADAMS

JANUARY 1993

Sensitivity Studies of In-Flight Black Liquor Combustion Using a Three-Dimensional Computer Model

R.R. Horton, D.J. Slayton, T.M. Grace, and T.N. Adams

Presented at the
1992 Annual AIChE Meeting
Miami Beach, FL
November 2–6, 1992

Sensitivity Studies of In-Flight Black Liquor Combustion Using a Three-Dimensional Computer Model

Robert R. Horton, Donald J. Slayton, Thomas M. Grace, and Terry N. Adams
Institute of Paper Science and Technology
575 14th St. NW
Atlanta, GA 30318

ABSTRACT

A three-dimensional recovery furnace computer model has been developed which describes the in-flight combustion behavior of black liquor. The model is based on fundamental parameters from heat and mass transfer theory, and empirical parameters that were determined in black liquor combustion experiments. This paper presents the results of sensitivity studies of key model parameters.

Model parameters that are studied include variables that are not known with a high degree of confidence such as gas emissivity and char gasification rate constants, and empirical parameters that include swelling factors and solids concentration at ignition which could vary between liquor sources or furnace conditions. The three dimensional geometry of the simulated furnace includes boundary conditions for four walls, a char bed, a bullnose, and an outlet. A realistic gas velocity field including recirculation regions is used for all simulations. Output from computer simulations includes an estimate of entrainment (carryover), wall and bed impacts, and characterizations of in-flight combustion behavior. Results of this study give insight into why different black liquors may burn differently.

INTRODUCTION

An accurate black liquor combustion model is central to the development of a generalized recovery boiler model which predict features of boiler operation using combustion and computational fluid dynamics theory. Several recent publications (1-10) discuss the development of recovery boiler models. Additional studies have been reported specifically on black liquor combustion models (11-14). Frederick, Hupa and others (7,12,13,14) have proposed the most recent black liquor combustion model based on laboratory combustion experiments which includes both fundamental heat and mass transfer theory as well as empirically determined model parameters. This model has been used as the basis for a recovery boiler simulation computer program developed at the Institute of Paper Science and Technology (15).

The purpose of this study is to examine the importance of key parameters within the black liquor combustion model using full three-dimensional boiler simulations. Earlier studies with regard to model accuracy and parameter sensitivity have been conducted with in two-dimensional geometries with simple, uniform flow fields and single droplets. The present study is the first to examine model parameter sensitivity using realistic, recirculating flow fields in a three dimensional geometry with black liquor sprays made up of thousands of drops. This approach shows which of the black liquor parameters are most important in overall combustion behavior and gives insight into why some liquors may burn differently than others.

Combustion Model

The black liquor combustion model used in this work is based on descriptions of the four stages of black liquor combustion: 1) drying, 2) pyrolysis, 3) char burning, and 4) inorganic smelt reactions. The model follows the methodology reported by Frederick (7) with modifications of the char burning model suggested by Grace (16). Heat and mass transfer relationships are used to predict the rates at which each of the combustion stages occur. Heat transfer calculations are based on a single, film resistance model. The trajectories of individual droplets are determined by a force balance using a coefficient of drag relationship and are influenced by swelling characteristics of the black liquor and gas flow patterns within the furnace (17). These trajectories dictate where mass and energy are exchanged between the gas and droplet phases and whether the droplets become entrained or fall to the char bed. Thus, these trajectories influence deposit formation in the superheater, corrosion locations, char bed formation, and the throughput capacity of the recovery boiler. Table 1 lists combustion model parameters examined in this paper.

Table 1. Parameters of Black Liquor Combustion Model Examined in Sensitivity Studies.

Parameter	Description
ε	Gas emissivity
DR_{drv}	Swelling Parameter During Drying
DR_{max}	Maximum Swelling (occurs at end of Pyrolysis)
S_i	Fraction of solids at ignition (defines onset of pyrolysis)
T_{max}	Maximum drop temperature during pyrolysis
X_{char}	Mass fraction of liquor solids that burns as char

Model parameters include gas emissivity, ε, which may vary depending on temperature and composition of the gas phase, along with five parameters that can be experimentally determined in a laboratory furnace, but which may vary between liquors. Base case values for the model parameters are listed in Table 2.

Table 2. Base Case Values for Model Parameters.

Parameter	Value
ε	0.4
DR_{drv}	1.6
DR_{max}	3.0
S_i	0.95
T_{max}	654°C
X_{char}	0.1

Base Case Furnace Description

Parameter sensitivity studies were conducted using a base case gas phase flow field determined by computational fluid dynamics simulation of isothermal flow in a 10m x 10m x 30m geometry described in Horton, et al. (12). An isometric view of half the boiler geometry is shown in Figure 1 with contours of velocity magnitude in a vertical plane. The base case simulation was chosen to represent typical operating conditions in a recovery furnace. A relatively wide spray pattern was specified, 140° wide total spray angle, with 57 discrete angles for initial droplets trajectories to represent a splash plate nozzle . Black liquor was injected at a slightly downward vertical angle of -10°. A mean diameter of 2.5 mm was used with a distribution of 20 droplet sizes that ranged from 0.932 mm to 4.823 mm. Mass flow rates were corrected to agree with a parabolic flow profile. A total of 1140 droplets (57 discrete angles x 20 discrete diameters) were used to represent a spray from each of four nozzles; one in the middle of each wall at 6 m elevation.

The recovery furnace computer simulations sum the combustion product mass transferred into each cell of an arbitrarily defined grid of cells. For the combustion rate simulations presented here, a uniform 30 x 30 x 60 grid was prescribed on the furnace geometry. Four output arrays contain the sum of mass transferred from all individual droplets according to the stage of combustion. Additional boundary arrays sum the droplet mass that strikes the walls for each of the four combustion stages. The current model does not consider in-flight reactions of smelt, so all inorganic mass in the original black liquor ends up on one of the boundaries: the char bed, one of the four walls, the bull nose, or the outlet.

The in-flight combustion rate arrays are plotted using visualization software which displays three-dimensional perspective views of the data resembling color coded clouds. Each point of the cloud has an intensity and location corresponding to the magnitude of mass transferred at that cell location with a color corresponding to each of the four stages of black liquor combustion. Options are available to change the perspective and view of the furnace in order to appreciate the three-dimensional nature of the results.

Approach

This sensitivity study involved modeling the in-flight combustion of black liquor sprays upon the input of certain combustion model parameters. The model parameter ranges studied in these trials are specified in Table 3.

Table 3. Values of Parameters Tested in Sensitivity Studies.

Parameter	Range of Values
ε	0.32 - 0.80
DR_{dry}	1.0 - 2.0
DR_{max}	2.0 - 4.0
S_i	0.7 - 1.0
T_{max}	600 - 800 °C
X_{char}	0.025 - 0.2

To determine the sensitivity of model parameters, a simulation was run at high and low values of parameter ranges listed in Table 3 while keeping all other model parameters at base case values. Each simulation was run using the base case black liquor spray and flow field described previously. Plots of char combustion clouds proved to be the most valuable in visually identifying qualitative differences in black liquor combustion behavior since differences in evaporation and pyrolysis would also affect location of char burning.

Base case combustion clouds for water, pyrolysis, and char combustion are shown in Figure 2. Relative rates of in-flight combustion with respect to vertical position in the furnace for the base case are shown in Figure 3. A plot of black liquor mass impacting the wall vs. elevation is shown for the base case in Figure 4. Figures similar to these along with predictions of entrainment (carryover) were used as model outputs for comparing parameter sensitivities.

For parameters where large sensitivities were observed, additional simulations were performed using intermediate parameter values within the range indicated in Table 3. This technique also allowed identification of nonlinearities. In an effort to understand the mechanisms by which the model parameters affect droplet combustion behavior, individual droplet trajectories were also examined.

RESULTS

Three dimensional char combustion cloud plots are shown in Figures 5-10 for high and low range values of each of the six model parameters studied. From these plots one can qualitatively observe the sensitivity of each parameter. Rate plots and wall impact plots for these cases are presented in Figures 11-34 allowing a more quantitative measure of sensitivity. Figures 35-40 show the effects of parameter values on predicted carryover. Sensitivities for all six parameters are summarized qualitatively in Table 4.

Table 4. Sensitivities of Model Parameters

Parameter	Sensitivity
ϵ	small
DR_{dry}	large
DR_{max}	moderate
S_i	small
T_{max}	small
X_{char}	moderate

The three most sensitive model parameters were DR_{dry}, X_{char}, and DR_{max}. This is apparent in the location of char combustion activity as well as rate, and wall impacts. In general, only DR_{dry} and X_{char} significantly affected the relative amounts of carryover. Other model parameters had only minor sensitivity in simulation output.

Radiative heat transfer accounted for roughly half of the total heat transfer to the droplet during drying and pyrolysis in the simulations reported here. However, gas emissivity did not have a large impact on combustion behavior. This is due to the fact that gas temperature, wall temperature, and char bed surface temperatures were similar; values were 1000°C, 800°C and 1000°C respectively. Gas emissivity is expected to be

more important only when large temperature differences exist between local gas temperature and other radiating surfaces near the droplet.

Solids at ignition, S_i, the model parameter that determines when the droplets progresses from the drying stage to the pyrolysis stage, did not have a big effect on overall combustion behavior. Neither did T_{max} which determines the end of pyrolysis and the beginning of char burning. These findings indicate that defining precisely when one stage of combustion ends and the next begins is not critical within reasonable ranges and that no additional experimental work is necessary to refine measurements of S_i and T_{max}.

Swelling

Both DR_{dry} and DR_{max} describe black liquor swelling, the first during drying and the second during pyrolysis. Both affected black liquor combustion behavior. Of the two, swelling during drying was more critical than swelling during pyrolysis in both overall combustion behavior and for individual droplet trajectories.

The char combustion cloud moved significantly higher in the furnace when DR_{dry} was raised from 1.0 (no swelling) to 2.0 (high swelling). Changes in DR_{max} had the opposite effect. When DR_{max} was increased from 2.0 to 4.0, the char combustion took place much lower in the furnace. Also noted was that for increasing values of DR_{dry}, there were increases in the amount of evaporation that occurred near the elevation of the liquor guns.

Examining the wall impact plots also shows that predictions are sensitive to DR_{dry} here as well. Varying DR_{dry} resulted in large shifts in the location and nature of the impacting black liquor. The combustion model predicts that as DR_{dry} increases, the relative amounts of combustion occurring on the walls greatly decreases. And as DR_{dry} is increased from 1.0 to 2.0, the relative amount of smelt carryover greatly decreases.

From these results alone it is not clear whether the sensitivity of combustion behavior to swelling (especially during evaporation) is due to a greater drag resulting in an alteration of trajectory, or an increase in surface area of the droplet resulting in higher heat transfer rates. In order to fully understand the effects of swelling during drying, individual droplet trajectories were studied for different values of DR_{dry}.

Figure 41 shows two dimensional trajectories of 1.5 mm droplets during the evaporation stage of combustion for three different degrees of swelling, DR_{dry} = 1.2, 1.6, and 2.0. These simulations were conducted in a uniform upward velocity of 3.3 m/s. Each data point is plotted at 0.05 sec. intervals. This plot shows that the trajectory during drying is altered very little by the degree of swelling, but the time to complete the drying stage can change significantly. This in turn determines where along its trajectory a droplet will begin to pyrolyze. This reasoning agrees with the heat transfer mechanism

for both convective and radiative heat transfer. An expression for the overall heat transfer rate to the droplet is given by:

$$\frac{dQ}{dt} = hA(T_g - T_d) + \sigma A(T_g^4 - T_d^4) \quad (1)$$

where: Q = heat
h = heat transfer coefficient
A = surface area of droplet
T = temperature of gas or droplet
σ = Stefan-Boltzmann constant

And since surface area of the droplet is given by:

$$A = \pi D_0^2 DR_{dry}^2 \quad (2)$$

we can expect heat transfer to be proportional to the square of swelling. An increase in droplet diameter also causes a slight reduction of the overall heat transfer coefficient (7), however this is not as significant as the change in surface area available for heat transfer.

Figure 42 shows the trajectories for 1.5 mm droplets for all three combustion stages; evaporation, pyrolysis, and char burning. Since black liquor droplets will tend to become entrained during pyrolysis, the endpoint of evaporation determines when the droplets diverge from the downward trajectories. Figure 43 shows droplet trajectories during evaporation for 2.5 mm droplets in an upward velocity field of 3.3 m/s. Again the main effect of swelling is to change the time required to complete the drying stage. The divergence of overall trajectories is more pronounced in recirculating flow fields. Figure 44 shows complete combustion trajectories for 2.5 mm droplets for three different values of DR_{dry} in a realistic flow field.

Comparing the results presented here with those published by Frederick, et al. (19) we note differences in the sensitivity of DR_{dry}. These differences can be explained entirely by the use of a one resistance (film-only) heat transfer model in this work, versus a two resistance (film and internal) heat transfer model in the work reported by Frederick, et al. There is good rationale for using either method. The one resistance model appears more accurate at predicting ignition times at furnace temperatures greater than 700°C (7), while the two resistance model should be a better approximation if accurate thermal conductivity properties are available for black liquor undergoing swelling in a high radiative heat transfer mode. More work is needed to explore the implications of differences between these two models.

Since S_i also helps to determine the time required to complete the drying stage, it was somewhat surprising, initially, to find that changes in this model parameter did not have as large an impact on combustion as swelling. The reason that S_i did not have the

same effect was that water not evaporated during drying due to a low value of S_i would contribute to a higher density during pyrolysis. This caused the droplet to continue along the same trajectory as it would have if S_i were set at a higher value. It was upon completion of pyrolysis when droplet size was greatest and droplet density lowest that droplets became entrained. This implies that the most important aspect of black liquor combustion to model accurately is the onset of the char burning stage and not so much the distinction between drying and pyrolysis.

Individual droplets were injected into the base case furnace model to further investigate the relationship between the high velocity central core and the carry-over decreases observed with increasing values of DR_{dry}. The trajectories of several of these droplets are illustrated in Figures 45 and 46. These trajectories illustrate how large and small droplets in a typical spray distribution respond to changes in swelling during drying.

For larger droplets, the reduced momentum and drying time associated with increasing values of DR_{dry} result in a critical entrained trajectory for those droplets that are fired directly toward the center of the furnace. Larger droplets fired at angles are not entrained regardless of swelling. Carryover is observed to increase with increased swelling for large droplets fired directly toward the central high upward velocity core.

For medium and small droplets, increases in DR_{dry} result in reduced carryover. Droplets that would become entrained in the central core at low swelling now burn more quickly and are deflected back against the furnace walls. In addition, droplets that were sprayed at wide angles are found to more frequently impact the upper furnace walls or char bed.

For the nominal spray distribution studied in this work, an increase in swelling during drying resulted in less overall carryover. However, course black liquor spray directed primarily toward the center of the furnace (typical of v-jet nozzles) might show an increase in carryover with more swelling.

The conclusion from inspection of individual trajectory simulations is that the degree of swelling influences the surface area of the droplet which in turn influences the rate of heat and mass transfer. Black liquor that does not swell much will not burn as quickly. Depending on the spray angle and droplet size, this may contribute to temperature profiles that reflect burning in a wider range in the furnace and more carryover. In contrast, droplets that do swell will burn more quickly, resulting in higher local temperatures and perhaps less carryover.

Char Burning

As char content was increased by raising X_{char} from 0.025 to 0.2, there is a significant upward shift in the char combustion cloud. This is an intuitive result since char burning is typically a longer stage of combustion than drying or pyrolysis and more

char extends that time. This allows the black liquor to be entrained longer before coalescing into a dense smelt bead. Higher degrees of carryover with increasing char content are therefore predicted. X_{char} did not affect the drying or pyrolysis stages to a large degree, which is expected. Preliminary experimental work (15) has shown that char content may be a function of furnace temperature, with higher temperatures resulting in less carbon mass surviving into the char burning stage. This would imply that higher temperatures would favor shorter char burning times even if kinetics were not a rate limiting step.

CONCLUSIONS

This study has shown that in-flight combustion model predictions show high to moderate sensitivity to three black liquor combustion model parameters. In order of sensitivity these parameters are DR_{dry}, X_{char}, and DR_{max}. Three other parameters, gas emissivity, ε, Solids at ignition, S_i, and maximum pyrolysis temperature, T_{max}, were relatively insensitive model parameters. The insensitivity of predicted combustion behavior to S_i indicates that it may be possible to simplify the drying and pyrolysis stages into a single stage of the model, with the potential for reducing the number of required input parameters.

Swelling during drying was found to be important in determining overall combustion behavior due to the effect it had on drying rate. The values of DR_{dry} not only affected the location and rate of combustion but also the carryover and final fate of black liquor droplets. The use of one-resistance versus two-resistance heat transfer models appears to affect the sensitivity of swelling. Because DR_{dry} is a sensitive parameter in these studies, further investigations are planned with both types of heat transfer models.

Char content during the char burning stage, X_{char}, affected the time required for char combustion. Higher char contents resulted in more combustion higher in the furnace. Swelling during pyrolysis, specified by DR_{max}, affected the rates of both pyrolysis and char burning stages of black liquor combustion. Higher swelling factors reduced the time for combustion and concentrated combustion activity lower in the furnace.

ACKNOWLEDGMENT

Funding for this project was provided by IPST member companies and the U.S. Department of Energy under contract DE-FG02-90CE40936.

REFERENCES

1. Williams, T.J. and Galtung, F.L., "A Mathematical Model of a Recovery Furnace", Proceedings ISA/75, Milwaukee, WI, 1975.

2. Merriam, R.L. Kraft, *ver. 2.0* - Computer Model of a Kraft Recovery Furnace, A.D. Little, Inc., Cambridge, MA, 1980.

3. Shiang, N.T. and Edwards, L.L., "Kraft Recovery Furnace Capacity and Efficiency Improvement", Tappi Int.Rec.Conf., 1985.

4. Shick, P.E., "Predictive Simulation of Recovery Furnace Processes on a Microcomputer", Kraft Recovery Operations Seminar, Orlando, FL., 1986.

5. Grace, T., Walsh, A., Jones, A., Sumnicht, D. and Farrington, T., "Three-Dimensional Mathematical Model of the Kraft Recovery Furnace", TAPPI Int. Chem. Rec. Conf., 1989.

6. Karvinen, R., Hyoty, P. and Siiskonen, P., "The Effect of Dry Solids Content on Recovery Boiler Furnace Behavior", Tappi J., 74, no. 12, pp. 171-177, 1991.

7. Frederick, W. J., "Combustion Processes in Black Liquor Recovery: Analysis and Interpretation of Combustion Rate Data and an Engineering Design Model", U. S. Dept. Energy Report DOE/CE/40637-T8 (DOE90012712), 1990.

8. Chapman, P. J.,S. G. Janik, and A. K. Jones, "Visualization of the Recovery Boiler FLow Fields Predicted by Computational Fluid Dynamics", Tappi J. 75, no. 3., pp. 133-138, 1992.

9. Horton, R. R., T. M. Grace, and T. N. Adams, "The Effects of Black Liquor Spray Parameters on Combustion Behavior in Recovery Furnace Simulations", TAPPI Int. Chem. Recovery Conf., 1992.

10. Abdullah, Z., M. Salcudean, P. Nowak, and I. Gartshore, "Investigation of Interlaced and Opposed Jet Arrangements for Recovery Furnaces", Tappi Engr. Conf. Proc. pp.103-121, 1992.

11. Clay, D. T., H. G. Semerjian, and A. Macek, "Black Liquor Combustion in a Laboratory Flow Reactor - Status Report One", TAPPI Eng. Conf. Proc., pp. 41-48, 1987.

12. Hupa, M., P. Solin, and P. Hyöty, "Combustion Behavior of Black Liquor Droplets", JPPS 13, no. 2: pp 67-72, 1987.

13. Frederick, W. J., K. C. Kulas, and D. T Clay, "Analysis of Black Liquor Single Droplet Combustion Data", Int. Chem. Recovery Conf. Proc., pp 81-88, 1989.

14. Frederick, W. J., T. Noopila, and M. Hupa, "Combustion Behavior of Black Liquor at High Solids Firing", TAPPI J. 74, no. 12, pp. 163-170, 1991.

15. Empie, H., Grace, T., Frederick, W., Horton, R., Nichols, K., Medvecz, P. and Verrill, C., Black Liquor Combustion, Report No. 1, DOE Contract No. DE-FG02-90CE40936, in press.

16. Grace, T. M., "Revised Char Burning Model", Personal Communication, Aug. 1992.

17. Walsh, A. R. and T. M. Grace, "TRAC: A Computer Model to Analyze the Trajectory and Combustion Behavior of Black Liquor Droplets", JPPS 15, no. 3, pp. 84-89, 1989.

18. Horton, R. R., "In-flight Black Liquor Combustion Modeling: A Parameter Sensitivity Study", Timberline Colloquium on Recovery Boiler Modeling, 1991.

19. Frederick, W. J., T. Noopila, and M. Hupa, "Swelling of Spent Pulping Liquor Droplets During Combustion", JPPS 17, no. 5, pp. 164-170, 1991.

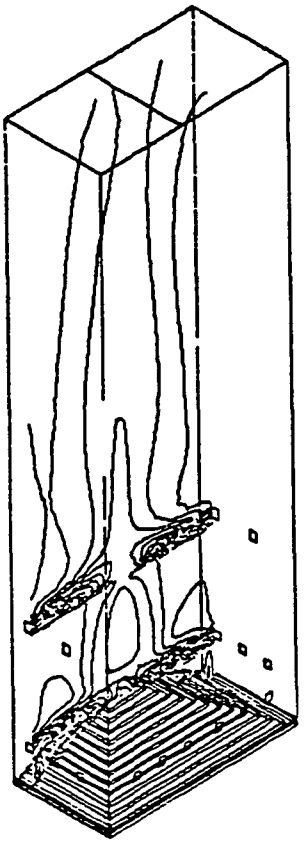

Figure 1. Isometric View of the Base Case Furnace Geometry.

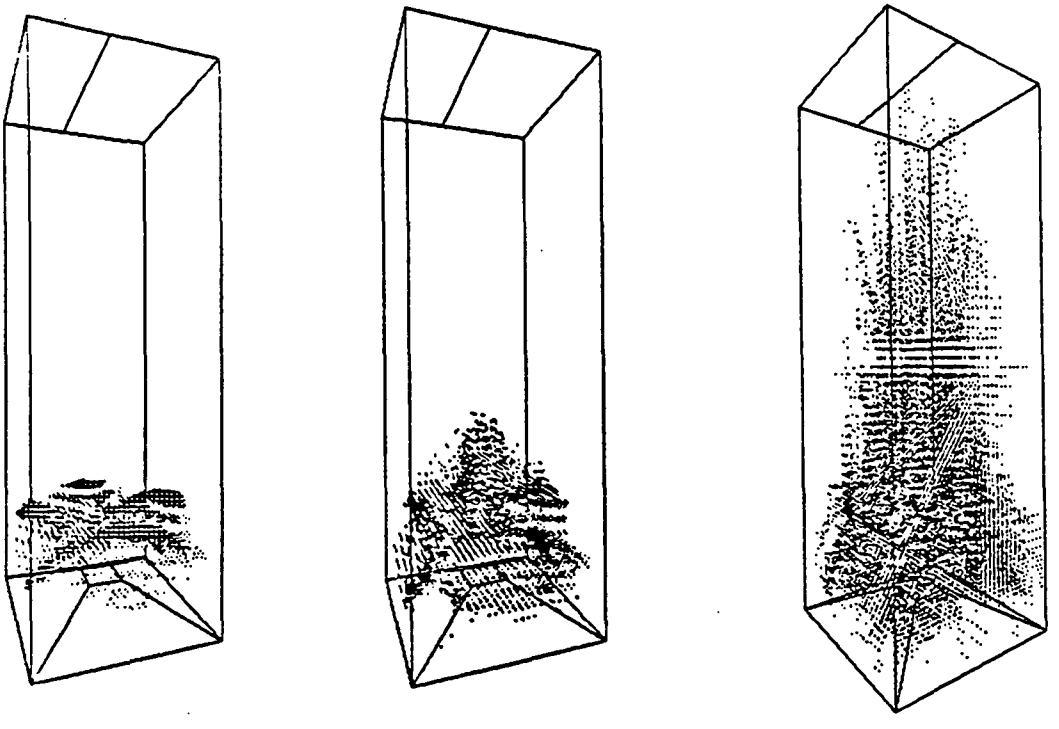

a) Evaporation b) Pyrolysis c) Char Burning

Figure 2. Three Stages of Black Liquor Combustion for the Base Case.

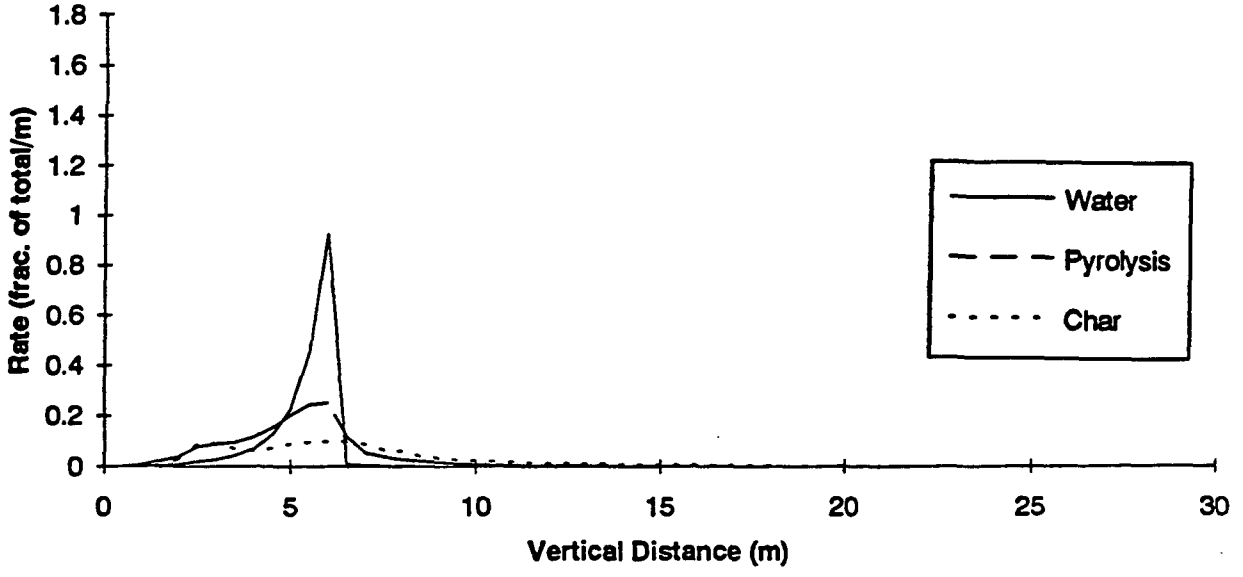

Figure 3. Local Rates of Mass Transfer by Vertical Position in the Furnace: Base Case.

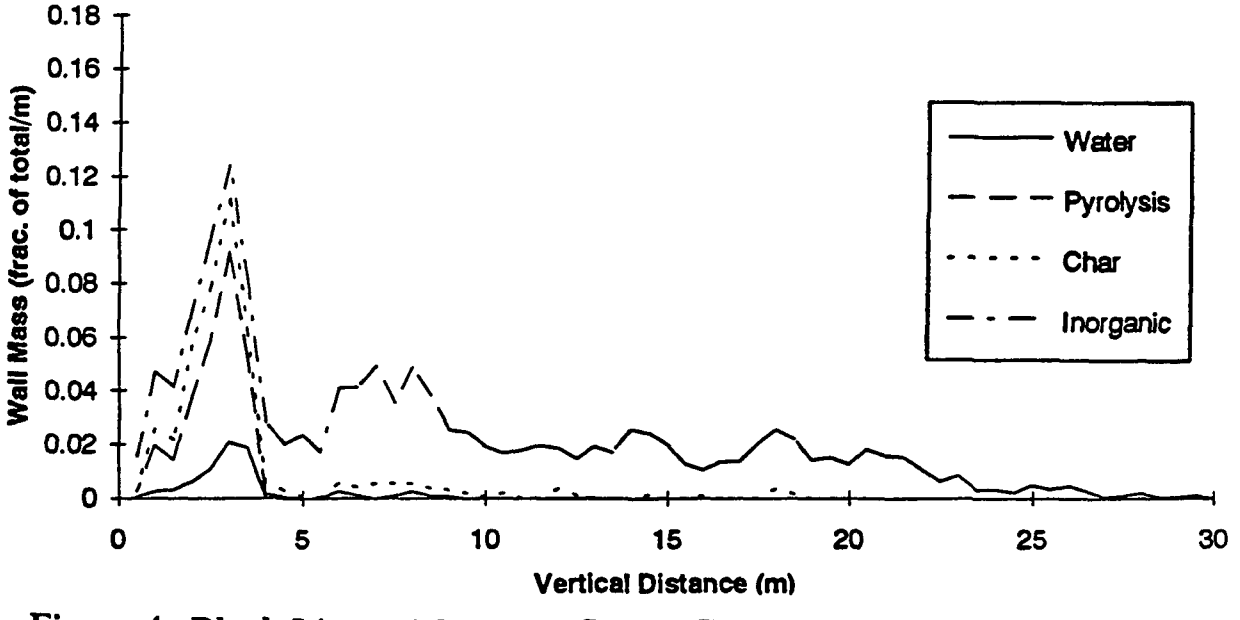

Figure 4. Black Liquor Mass that Strikes Furnace Walls: Base Case.

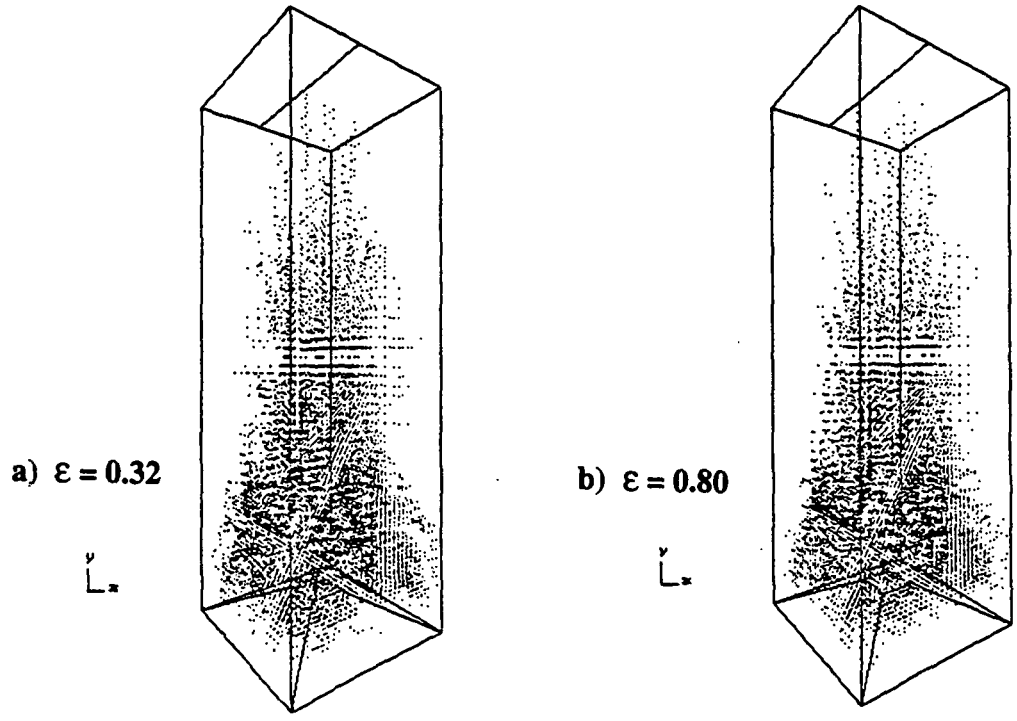

Figure 5. Three Dimentional Char Combustion Clouds for High and Low Values of Gas Emissivity.

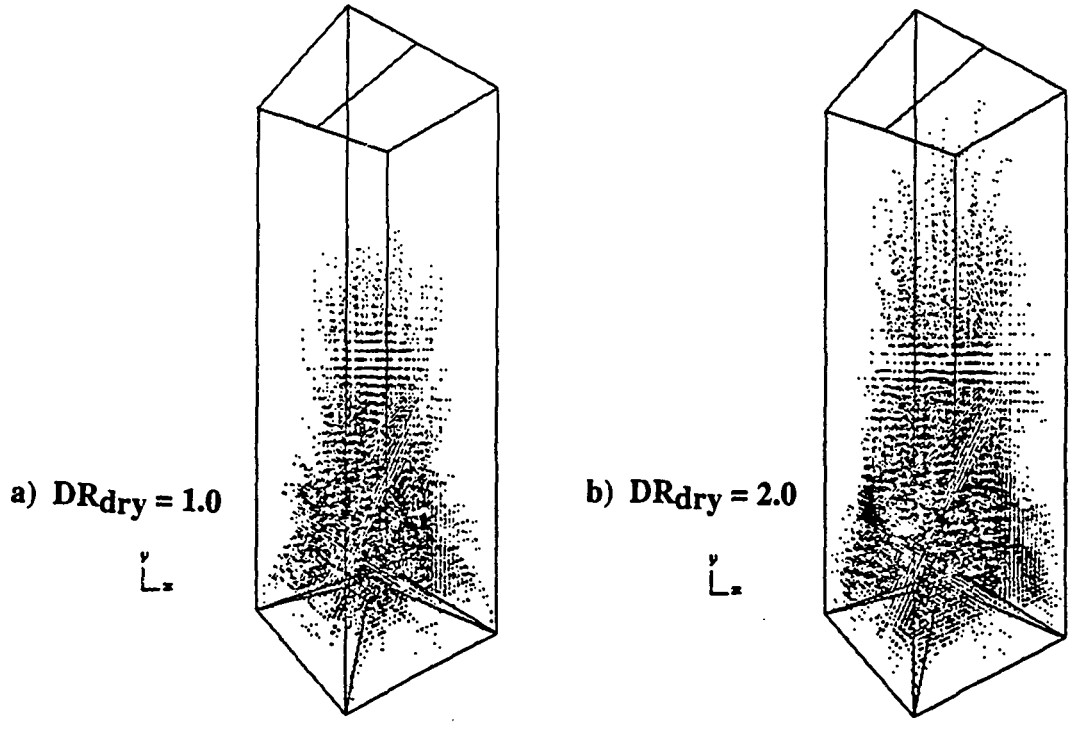

Figure 6. Three Dimentional Char Combustion Clouds for High and Low Values of the Swelling Parameter During Drying.

a) $DR_{max} = 2.0$

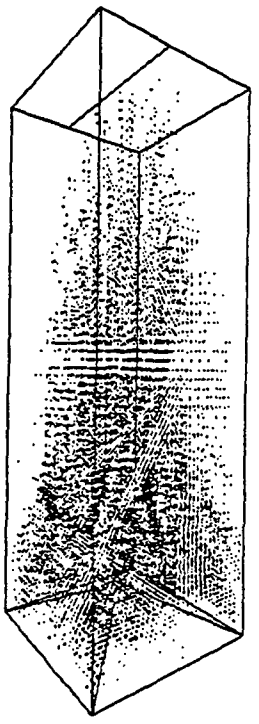

b) $DR_{max} = 4.0$

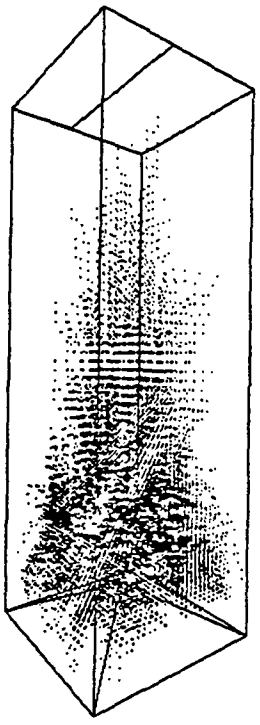

Figure 7. Three Dimentional Char Combustion Clouds for High and Low Values of Maximum Swelling.

a) $S_i = 0.7$

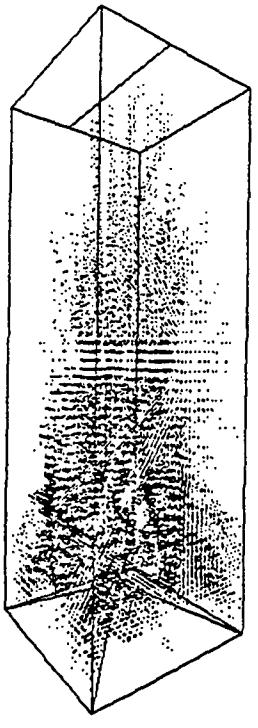

b) $S_i = 1.0$

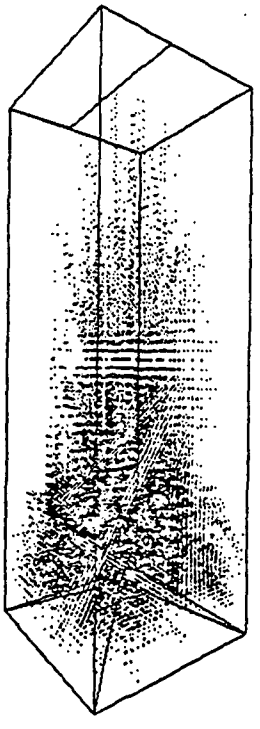

Figure 8. Three Dimentional Char Combustion Clouds for High and Low Values of the Percent Solids at Ignition.

a) $T_{max} = 600^{\circ}$ C

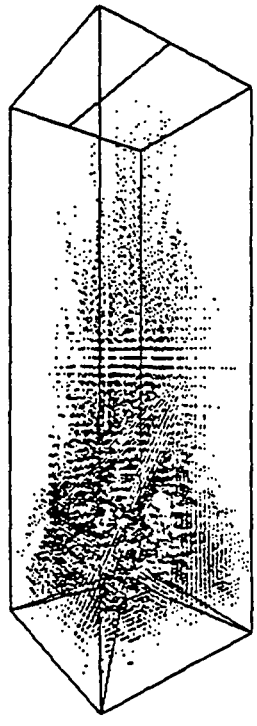

b) $T_{max} = 800^{\circ}$ C

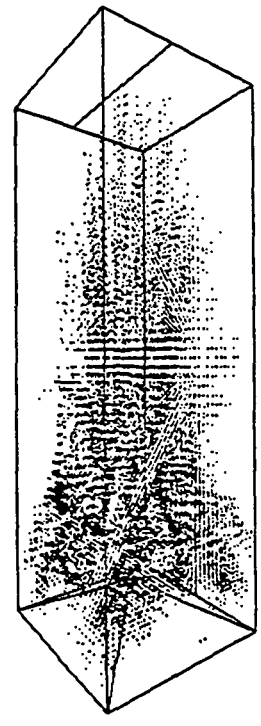

Figure 9. Three Dimentional Char Combustion Clouds for High and Low Values of the Maximum Drop Temperature During Pyrolysis.

a) $X_{char} = 0.025$

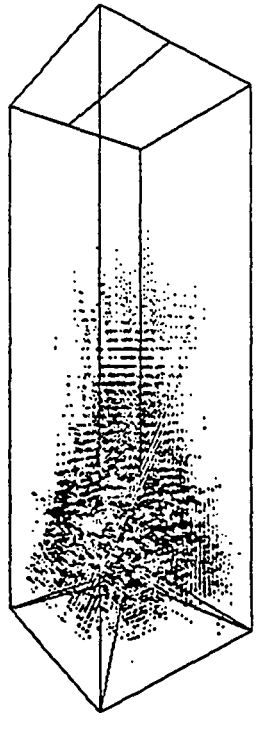

b) $X_{char} = 0.2$

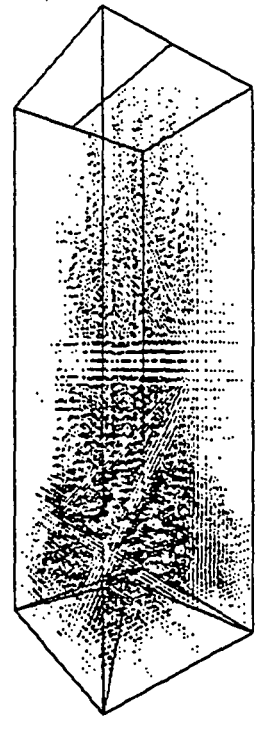

Figure 10. Three Dimentional Char Combustion Clouds for High and Low Values of the Mass Fraction of Liquor Solids that Burns as Char.

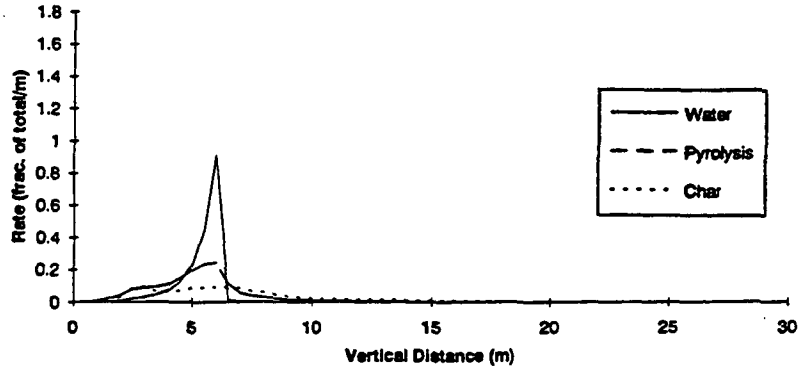

Figure 11. Local Rates of Mass Transfer by Vertical Position in the Furnace: $\varepsilon = 0.32$.

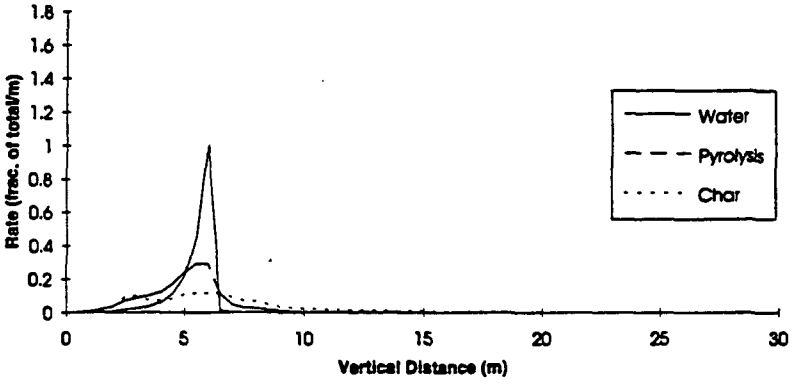

Figure 12. Local Rates of Mass Transfer by Vertical Position in the Furnace: $\varepsilon = 0.80$.

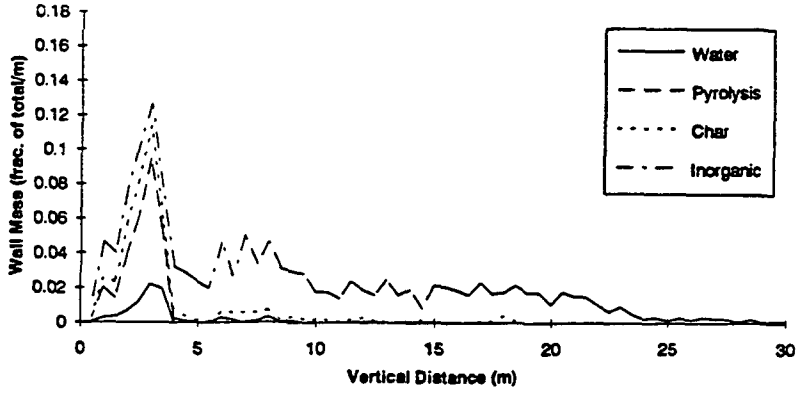

Figure 13. Black Liquor Mass that Strikes Furnace Walls: $\varepsilon = 0.32$.

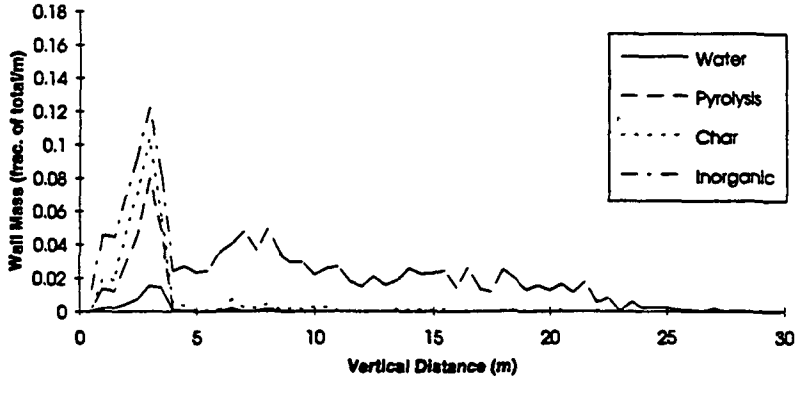

Figure 14. Black Liquor Mass that Strikes Furnace Walls: $\varepsilon = 0.80$.

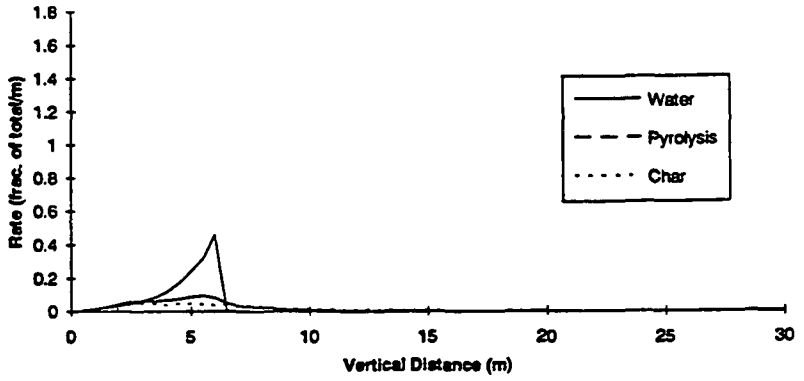

Figure 15. Local Rates of Mass Transfer by Vertical Position in the Furnace: $DR_{dry} = 1.0$.

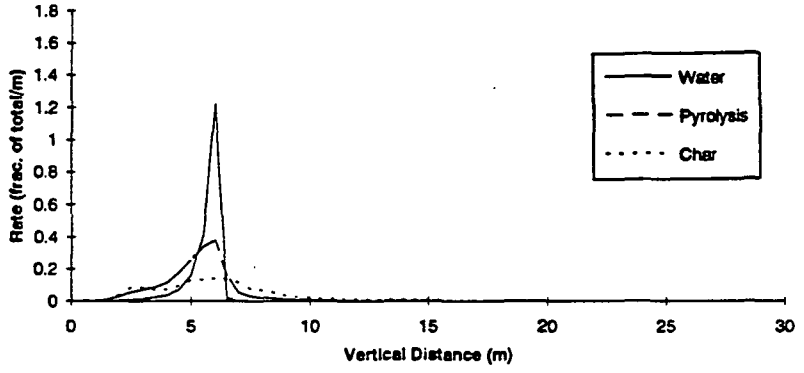

Figure 16. Local Rates of Mass Transfer by Vertical Position in the Furnace: $DR_{dry} = 2.0$.

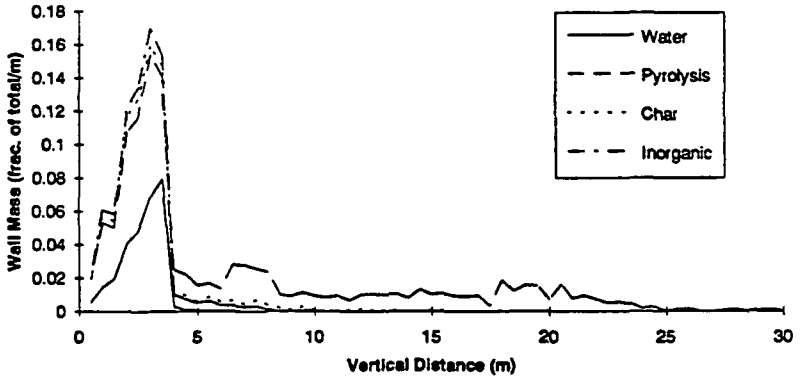

Figure 17. Black Liquor Mass that Strikes Furnace Walls: $DR_{dry} = 1.0$.

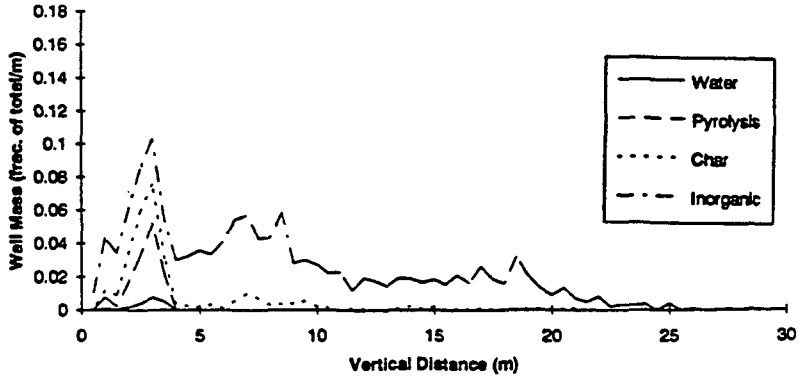

Figure 18. Black Liquor Mass that Strikes Furnace Walls: $DR_{dry} = 2.0$.

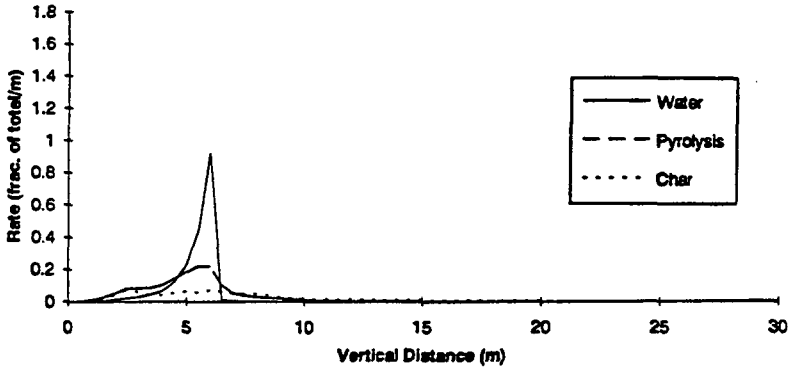

Figure 19. Local Rates of Mass Transfer by Vertical Position in the Furnace: $DR_{max} = 2.0$.

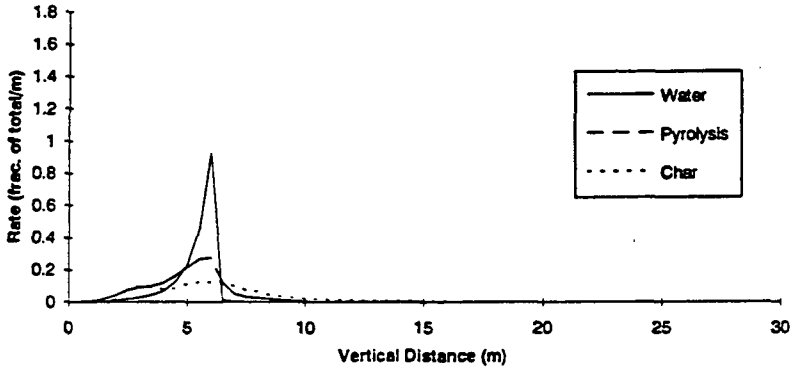

Figure 20. Local Rates of Mass Transfer by Vertical Position in the Furnace: $DR_{max} = 4.0$.

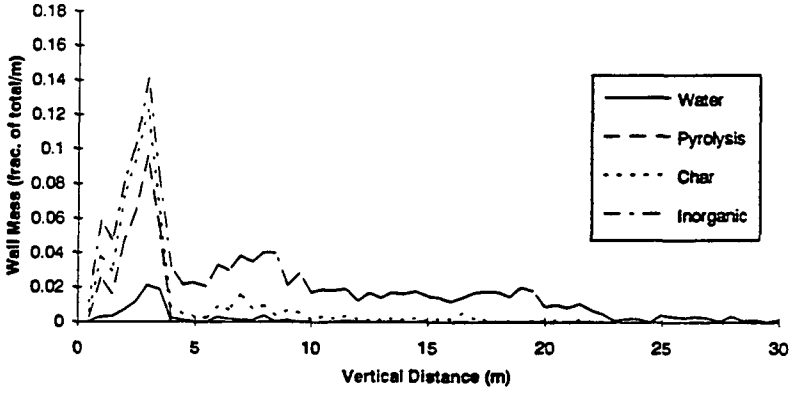

Figure 21. Black Liquor Mass that Strikes Furnace Walls: $DR_{max} = 2.0$.

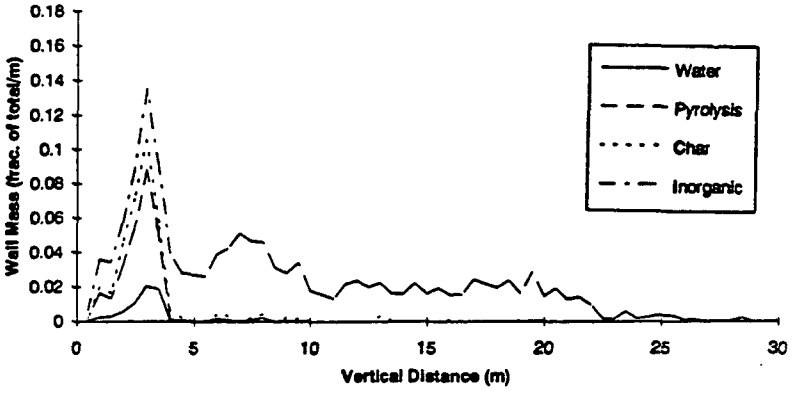

Figure 22. Black Liquor Mass that Strikes Furnace Walls: $DR_{max} = 4.0$.

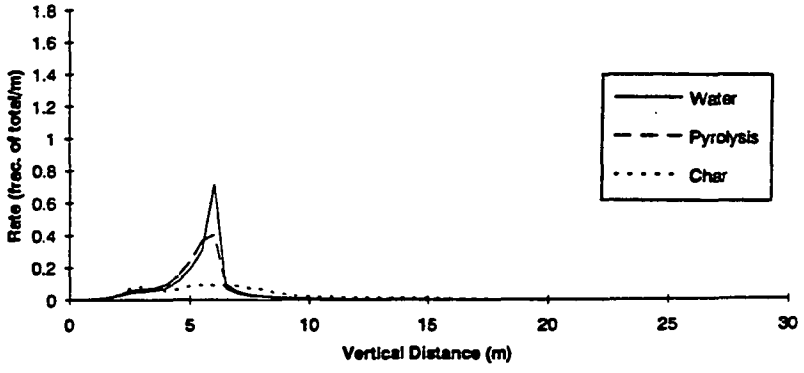

Figure 23. Local Rates of Mass Transfer by Vertical Position in the Furnace: $S_j = 0.7$.

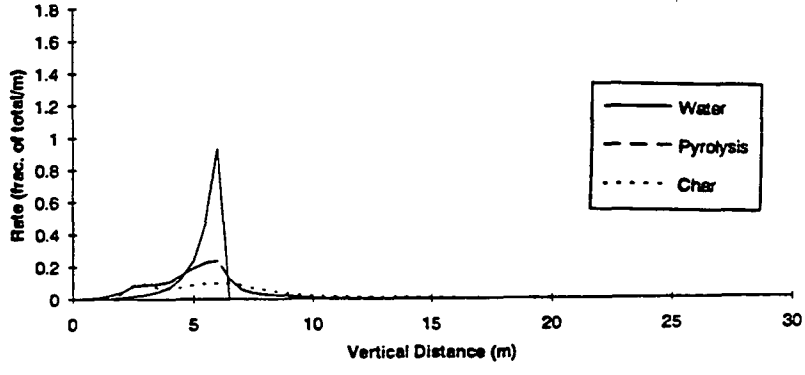

Figure 24. Local Rates of Mass Transfer by Vertical Position in the Furnace: $S_j = 1.0$.

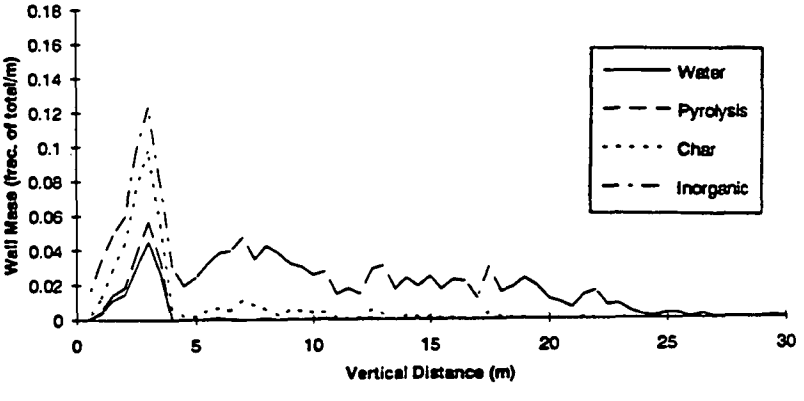

Figure 25. Black Liquor Mass that Strikes Furnace Walls: $S_j = 0.7$.

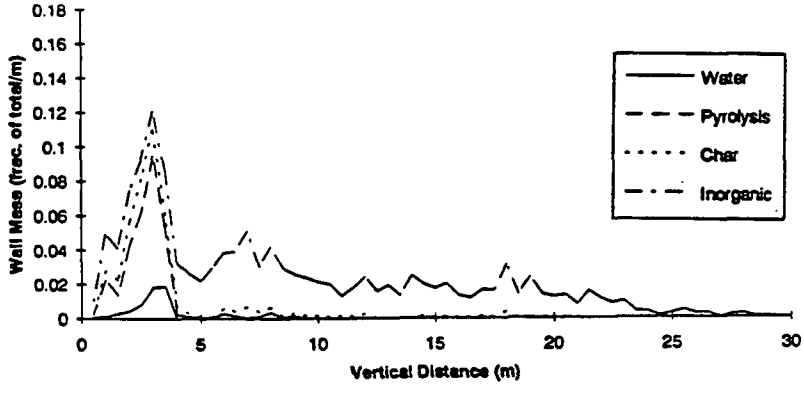

Figure 26. Black Liquor Mass that Strikes Furnace Walls: $S_j = 1.0$.

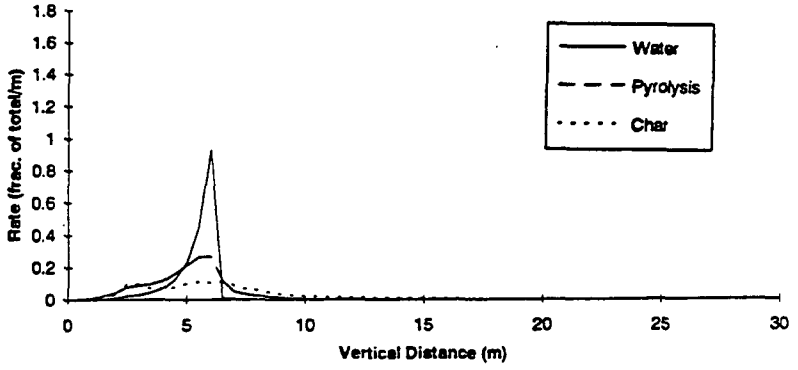

Figure 27. Local Rates of Mass Transfer by Vertical Position in the Furnace: $T_{max} = 600°C$.

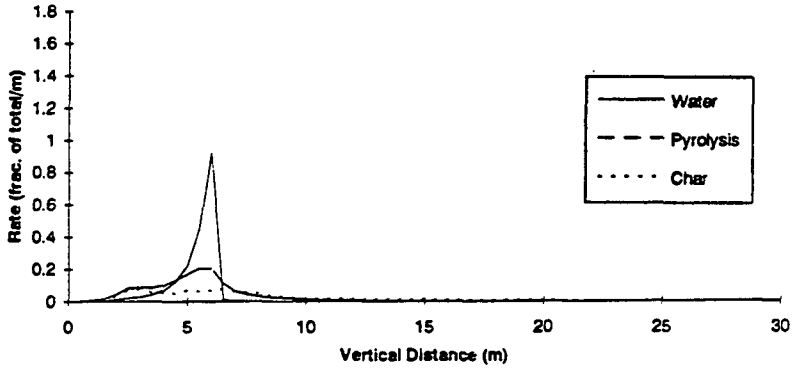

Figure 28. Local Rates of Mass Transfer by Vertical Position in the Furnace: $T_{max} = 800°C$.

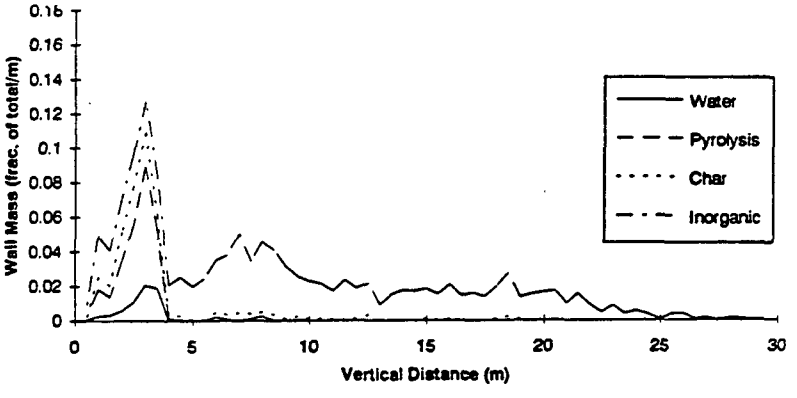

Figure 29. Black Liquor Mass that Strikes Furnace Walls: $T_{max} = 600°C$.

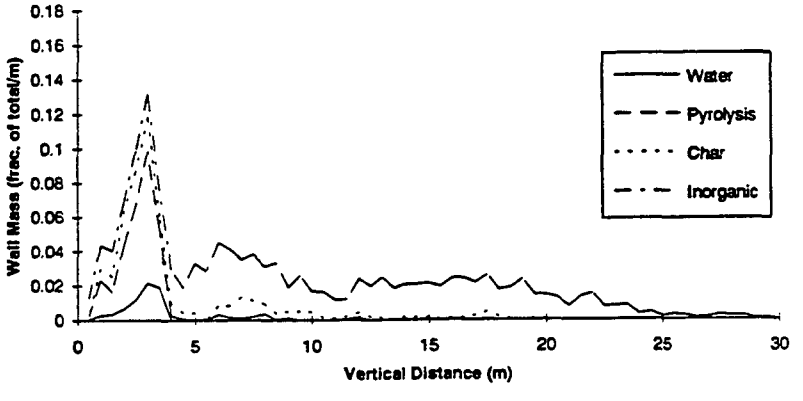

Figure 30. Black Liquor Mass that Strikes Furnace Walls: $T_{max} = 800°C$.

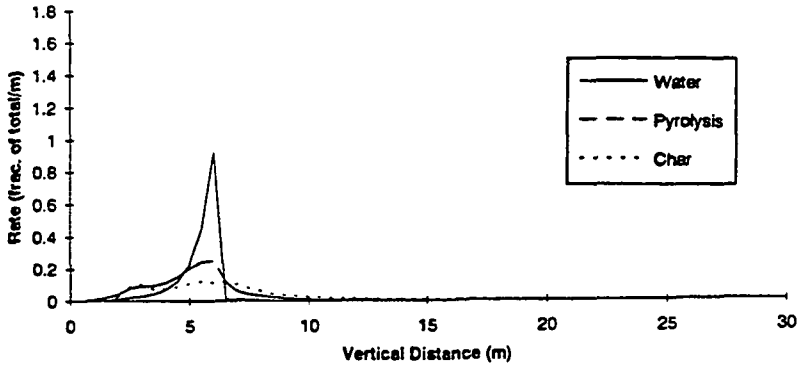

Figure 31. Local Rates of Mass Transfer by Vertical Position in the Furnace: $X_{char} = 0.025$.

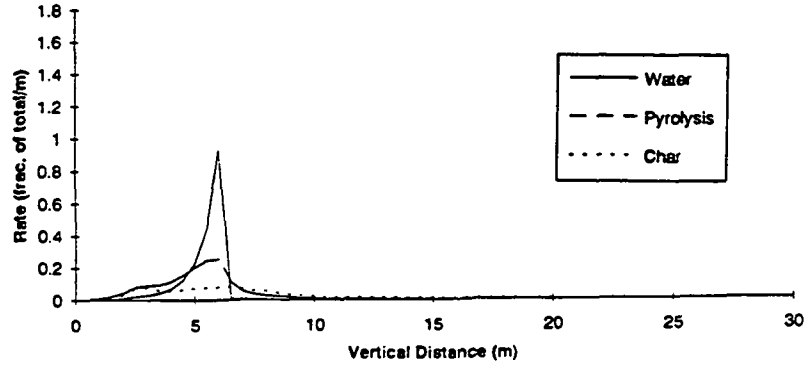

Figure 32. Local Rates of Mass Transfer by Vertical Position in the Furnace: $X_{char} = 0.2$.

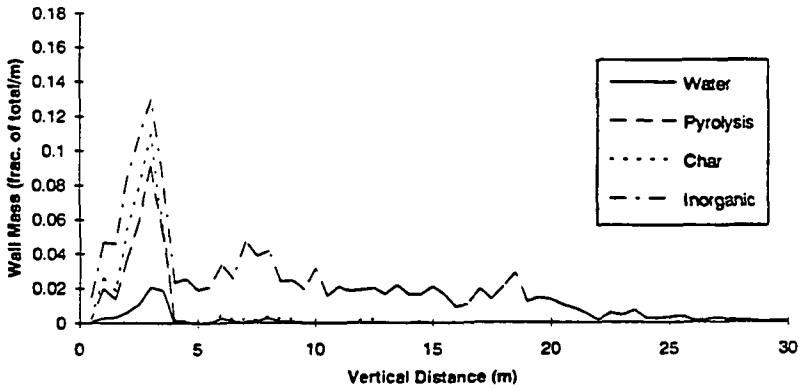

Figure 33. Black Liquor Mass that Strikes Furnace Walls: $X_{char} = 0.025$.

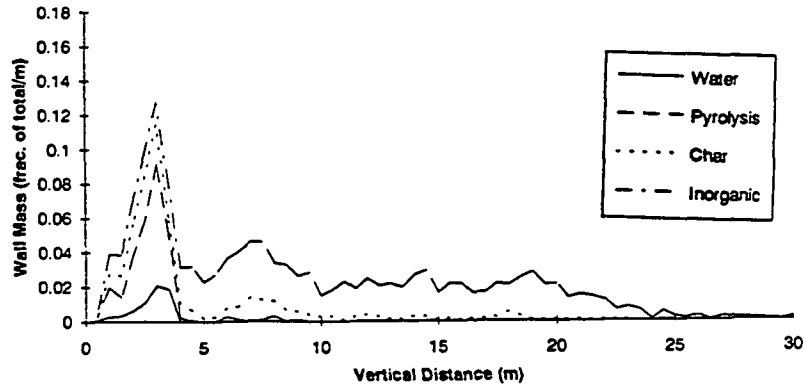

Figure 34. Black Liquor Mass that Strikes Furnace Walls: $X_{char} = 0.2$.

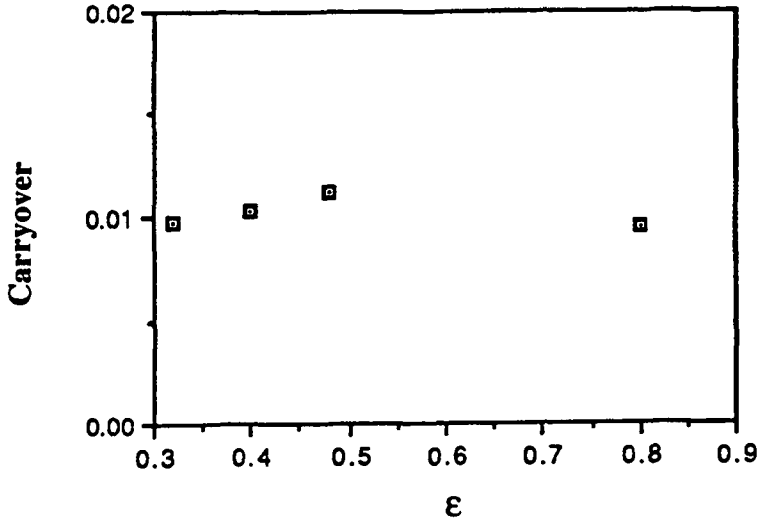

Figure 35. Smelt Carryover vs. ε.

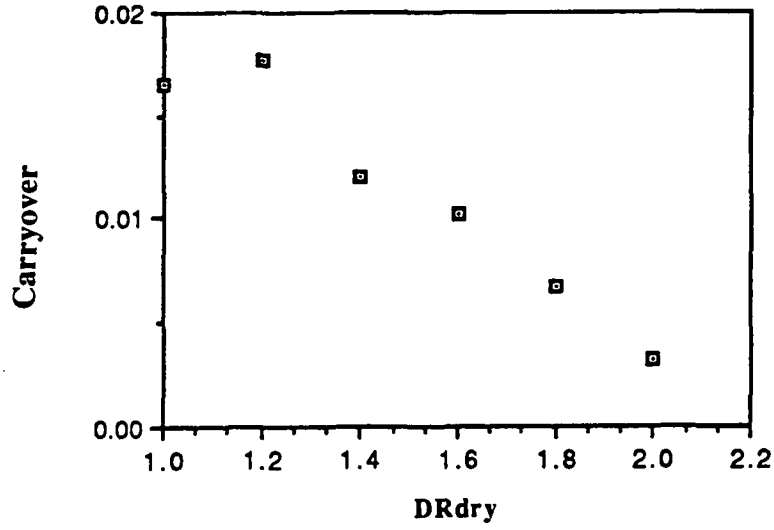

Figure 36. Smelt Carryover vs. DR_{dry}.

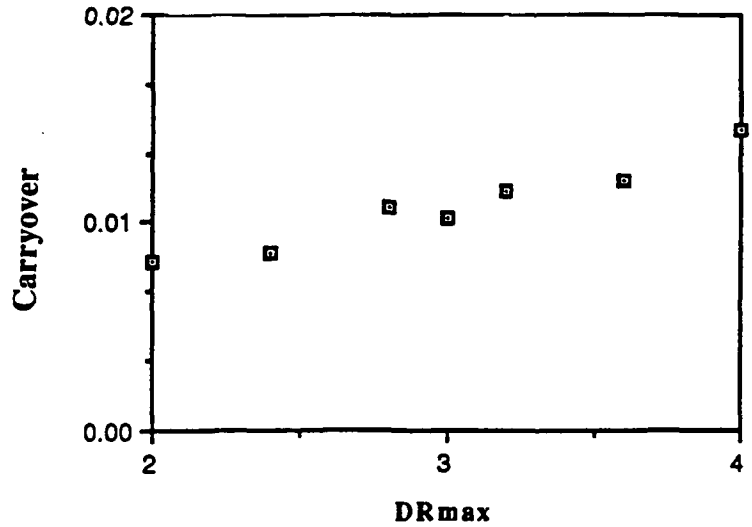

Figure 37. Smelt Carryover vs. DR_{max}.

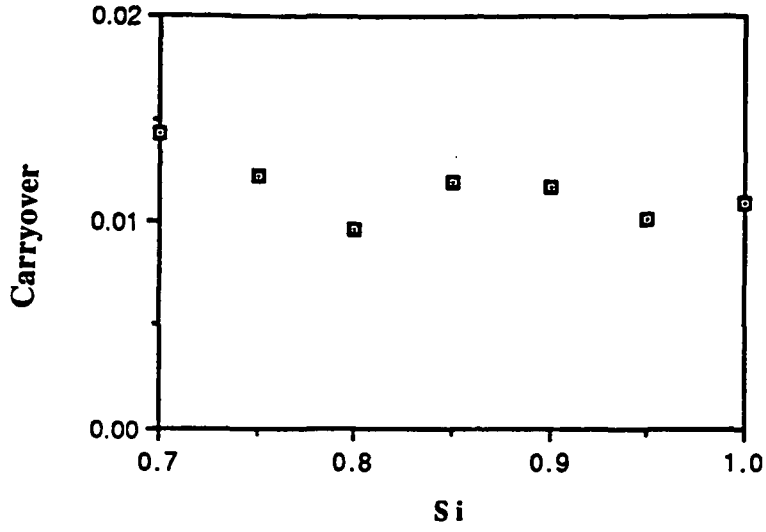

Figure 38. Smelt Carryover vs. S_i.

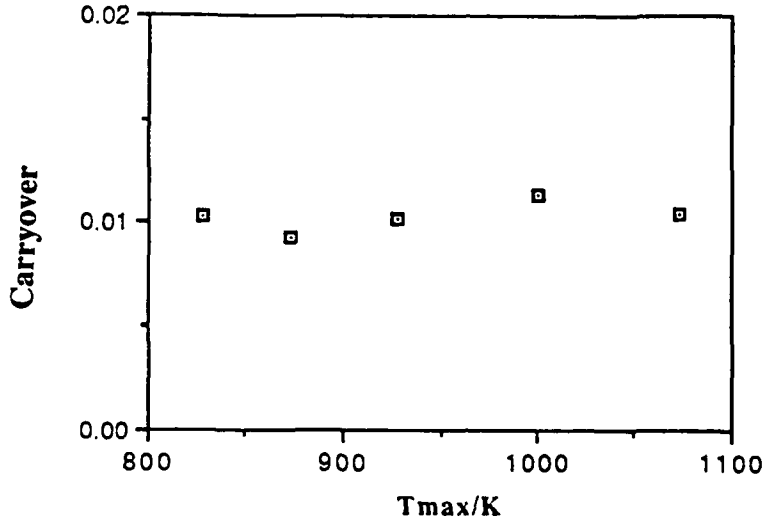

Figure 39. Smelt Carryover vs. T_{max}.

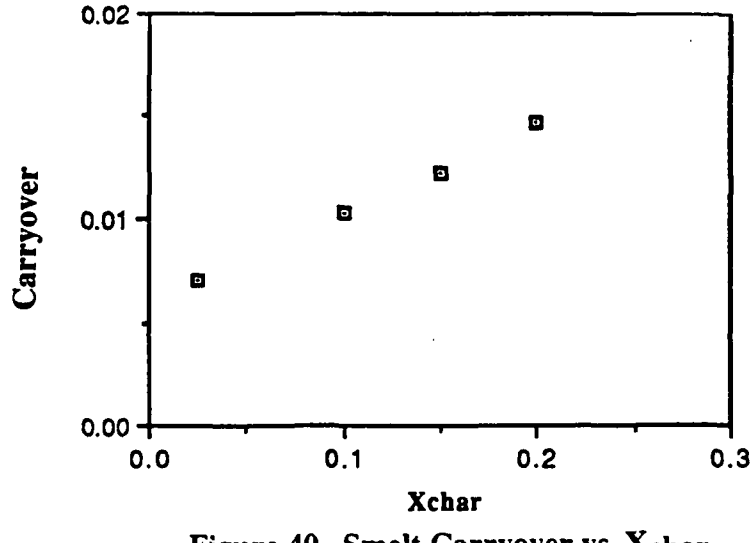

Figure 40. Smelt Carryover vs. X_{char}.

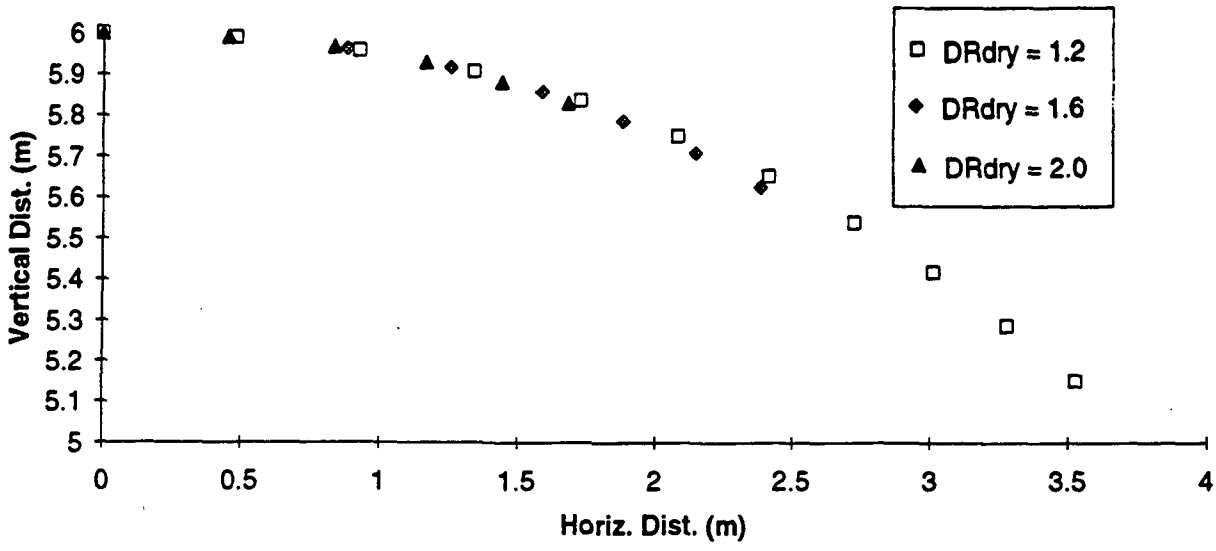

Figure 41. Trajectories for 1.5 mm Droplets for Three Swelling Ratios During Evaporation in a Uniform Upward Velocity of 3.3 m/s.

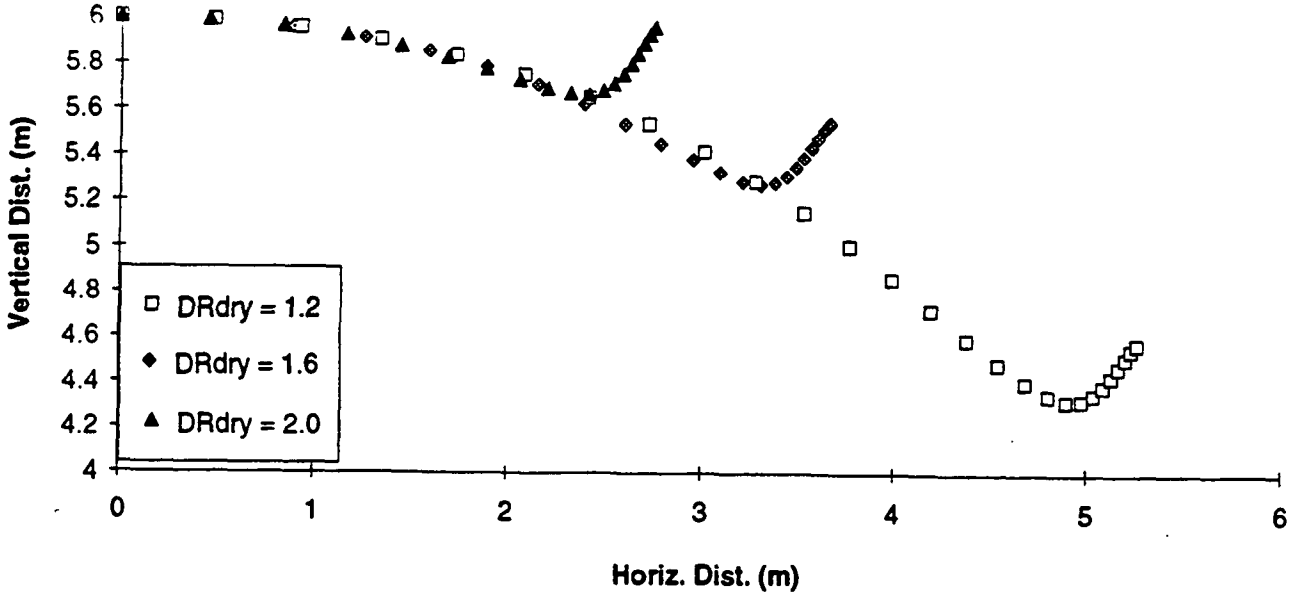

Figure 42. Trajectories of 1.5 mm Droplets for Three Swelling Ratios - Complete Combustion; Uniform Upward Velocity of 3.3 m/s.

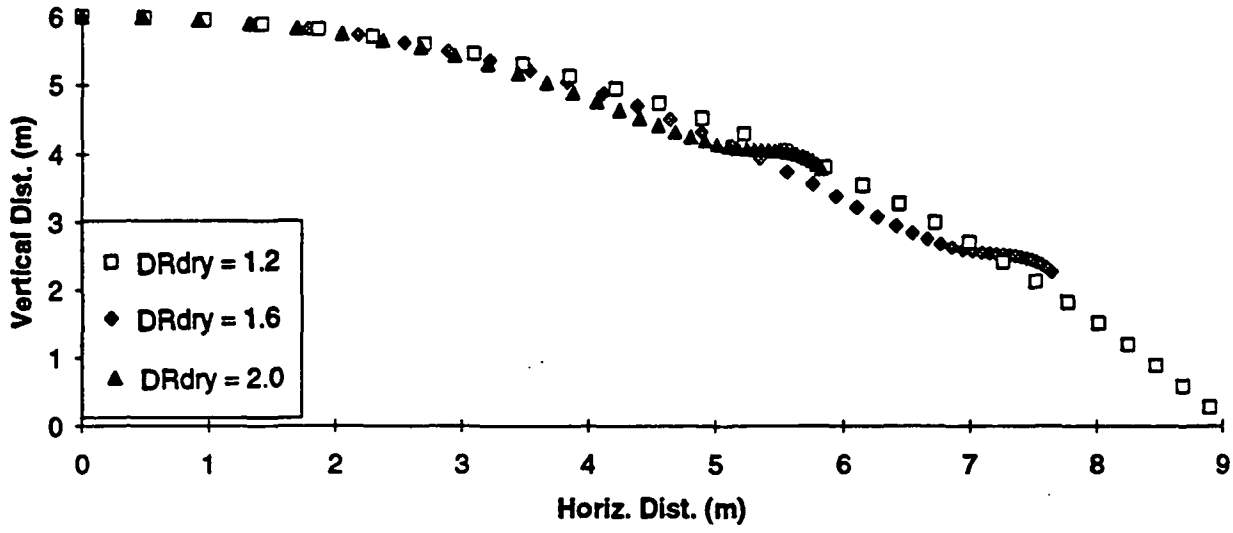

Figure 43. Trajectories of 2.5 mm Droplets During Evaporation in a Uniform Upward Velocity of 3.3 m/s.

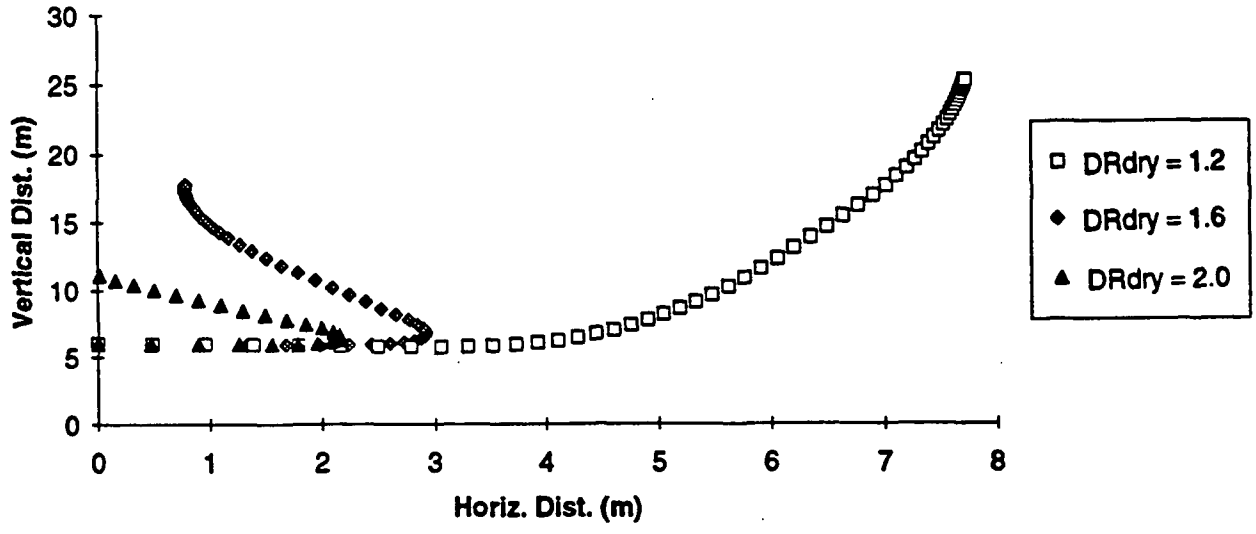

Figure 44. Trajectories of 2.5 mm Droplets - Complete Combustion in a Realistic Velocity Field.

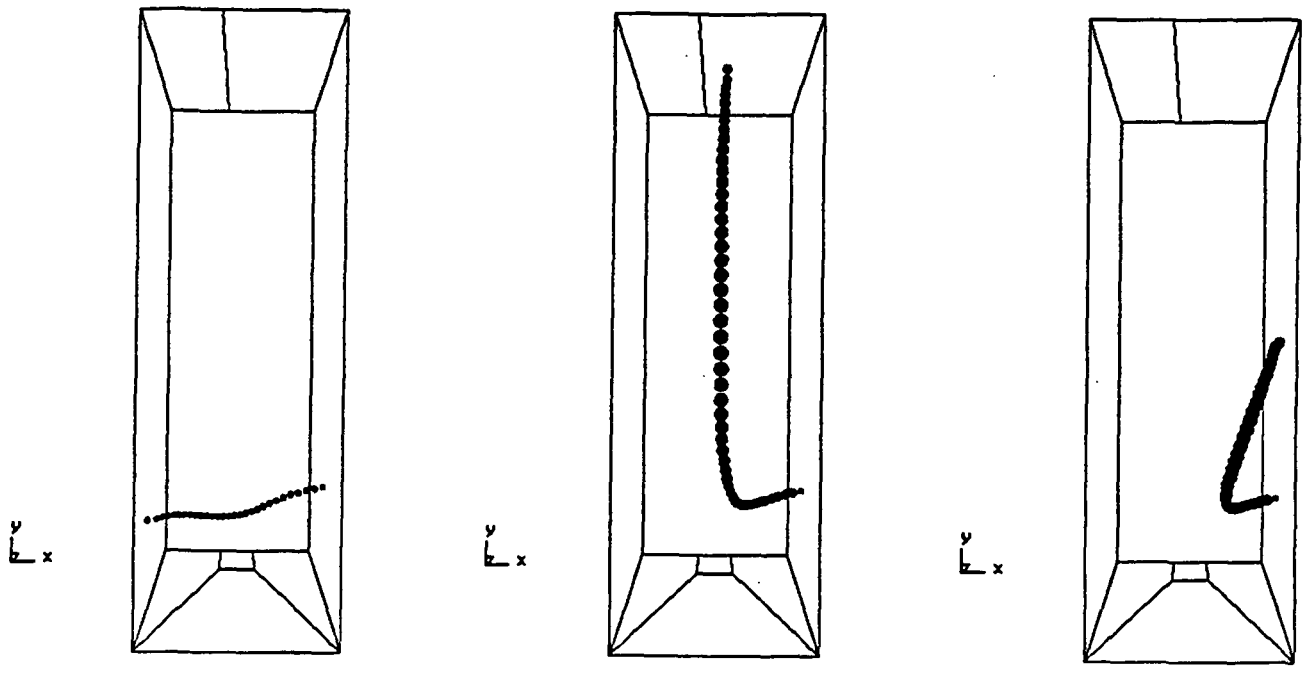

a) $DR_{dry} = 1.0$ b) $DR_{dry} = 1.6$ c) $DR_{dry} = 2.0$

Figure 45. Full Combustion Trajectories for Droplets Fired Towards the Center of the Furnace with Different Values for the Swelling Parameter During Drying. Side View.

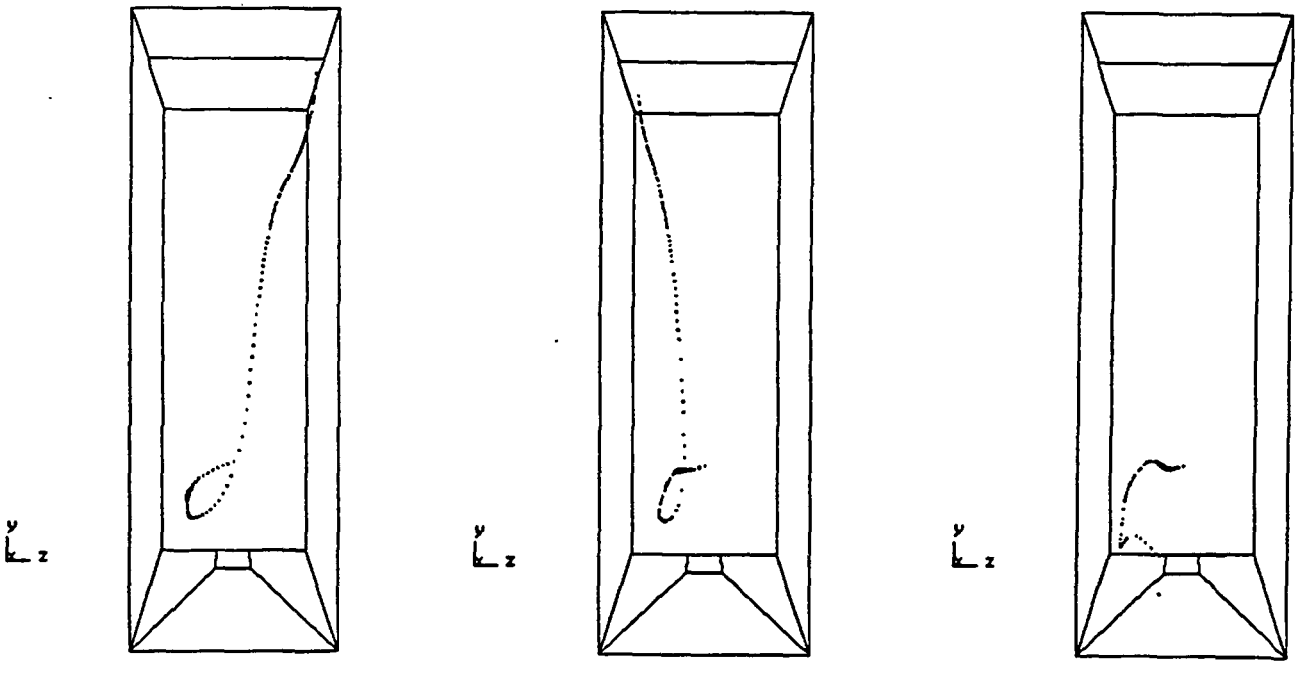

a) $DR_{dry} = 1.0$ b) $DR_{dry} = 1.6$ c) $DR_{dry} = 2.0$

Figure 46. Full Combustion Trajectories for Droplets in Recirculating Flow Fields with Different Values for the Swelling Parameter During Drying. Front View.